

Weak Lensing of Galaxy Clusters in MOND

Ryuichi Takahashi¹ and Takeshi Chiba²

¹ *Department of Physics and Astrophysics, Nagoya University, Chikusa-ku Nagoya 464-8602, Japan*

² *Department of Physics, College of Humanities and Sciences, Nihon University, Tokyo 156-8550, Japan*

ABSTRACT

We study weak gravitational lensing of galaxy clusters in terms of the MOND (MODified Newtonian Dynamics) theory. We calculate shears and convergences of background galaxies for three clusters (A1689, CL0024+1654, CL1358+6245) and the mean profile of 42 SDSS (Sloan Digital Sky Survey) clusters and compare them with observational data. The mass profile is modeled as a sum of X-ray gas, galaxies and dark halo. For the shear as a function of the angular radius, MOND predicts a shallower slope than the data irrespective of the critical acceleration parameter g_0 . The dark halo is necessary to explain the data for any g_0 and for three interpolation functions. If the dark halo is composed of massive neutrinos, its mass should be heavier than 2 eV. However the constraint still depends on the dark halo model and there are systematic uncertainties, and hence the more careful study is necessary to put a stringent constraint.

Subject headings: cosmology: theory – galaxies: clusters: individual (A1689, CL0024+1654, CL1358+6245) – gravitation – gravitational lensing

1. Introduction

MOND (MODified Newtonian Dynamics) ¹ is a theoretical alternative to Newtonian dynamics, proposed by Milgrom (1983). The theory itself strengthens gravitational force at large distances (or small accelerations) to explain galactic dynamics without dark matter. The equation of motion is changed if the acceleration is lower than the critical value $g_0 \simeq 1 \times 10^{-8} \text{cm/s}^2$. It is well known that this theory can explain galactic rotation curves with only one free parameter: the mass-to-light ratio (see review Sanders & McGaugh 2002). There are two motivations to study such an alternative theory: (i) General Relativity (GR) has not been tested accurately at much larger scale than 1 AU (ii) dark matter particles have not been directly detected and their nature still eludes us. Under these circumstances, several authors have recently studied alternative theories to GR (e.g. Aguirre 2003).

Bekenstein (2004) recently proposed a rel-

ativistic covariant formula of MOND (called TeVeS) by introducing several new fields and parameters. Following this, many authors began discussing relativistic phenomena such as parameterised Post-Newtonian formalism in the solar system (Bekenstein 2004), gravitational lensing (e.g. Zhao et al. 2006), cosmic microwave background and large scale structure of the Universe (Slosar et al. 2005; Skordis 2005; Skordis et al. 2006; Dodelson & Liguori 2006). In this paper, we discuss weak gravitational lensing of galaxy clusters.

Weak lensing provides an important observational method with which to test MOND. This is because weak lensing probes the lens potential outside of the Einstein radius, $r_E \sim (MD)^{1/2} \simeq 150 \text{kpc} (M/10^{14} M_\odot)^{1/2} (D/H_0^{-1})^{1/2}$, where M is the lens mass and D is the distance to the source. The gravitational law changes outside the MOND radius, $r_M = (M/g_0)^{1/2}$, where the acceleration is less than g_0 . Since $g_0 \approx H_0/6$, the Einstein radius r_E is a few times smaller than the MOND radius r_M , by a factor 2 at least, in the cosmological situation. Hence, we can test the MOND-gravity regime by weak lensing.

¹The phrase MOND is used here to refer to modified Newtonian gravity models without any dark matter.

Weak lensing is superior to X-rays as a means of probing the outer region of clusters. The lensing signal (strength of the shear) is proportional to the surface density Σ . On the other hand, the X-ray luminosity is proportional to the density squared ρ^2 and hence X-rays can probe the inner regions of clusters. Hence, the outer region of the clusters can be probed with weak lensing.

The gravitational lensing in MOND has been studied by many authors. Before Bekenstein proposed the relativistic formula, some assumptions were made² to calculate the lensing quantities (Qin et al. 1995; Mortlock & Turner 2001a; 2001b; White & Kochanek 2001; Gavazzi 2002). Just after Bekenstein's proposal, Chiu et al. (2006) and Zhao et al. (2006) first studied the lensing in detail and tested MOND with strong lensing data of galaxies. Zhao and his collaborators studied the gravitational lens statistics (Chen & Zhao 2006) and investigated a non-spherical symmetric lens (Angus et al. 2006). Recently, Clowe et al. (2006) indicated that a merging cluster 1E 0657-558 cannot be explained by MOND because the weak lensing mass peak is 8σ spatial offset from the baryonic peak (= mass peak of X-ray gas). However, Angus et al. (2007) noted that MOND can explain the data if the neutrino halo is included (see also Feix et al. 2007). Furthermore, the high observed collision velocity of the bullet clusters (shock velocity of $\sim 4700\text{km/s}$) is more readily obtained in MOND than CDM (Angus & McGaugh 2007).

Jee et al. (2007) recently found a ring like dark matter structure at $\theta \sim 75''$ in CL0024+1654 by analysing strong and weak lensing data. They suggested that the ring was formed by the line-of-sight collision of two clusters, like the bullet cluster 1E 0657-558. Just after their discovery, Famaey et al. (2007) noted that MOND can easily explain the density of the ring by adding the massive neutrino of 2 eV.

In this paper, we study three clusters (A1689, CL0024+1654, CL1358+6245) and mean profile of 42 SDSS (Sloan Digital Sky Survey) clusters. We calculate shears and convergences for these clusters and compare them with the observational

data. We perform a χ^2 fit of the data to give a constraint on the dark halo profile and the neutrino mass. Throughout this paper, we use the units of $c = G = 1$.

2. Basics

We briefly review the basics of gravitational lensing based on the relativistic MOND theory for a spherically symmetric lens model. Detailed discussions are given in Bekenstein (2004) and Zhao et al. (2006).

When a light ray passes through a lens with the impact parameter b , the deflection angle is

$$\alpha(b) = 2b \int_{-\infty}^{\infty} dl \frac{g(r)}{r}, \quad (1)$$

where l is the distance along the light path and r is the distance from the lens center, $r = \sqrt{l^2 + b^2}$ (see Fig.1).

The gravitational force due to the lens is

$$\tilde{\mu}(g/g_0)g(r) = g_N(r) = \frac{M(< r)}{r^2}, \quad (2)$$

where g_N is the usual Newtonian acceleration and $M(< r)$ is the lens mass enclosed inside a radius r . We use a standard interpolation function³ $\tilde{\mu}(x) = x/\sqrt{1+x^2}$ with $g_0 = 1 \times 10^{-8}\text{cm s}^{-2}$. Then, $\tilde{\mu}(x) = 1$ (i.e. $g = g_N$) for $g \gg g_0$, while $\tilde{\mu}(x) = x$ (i.e. $g = \sqrt{g_N g_0}$) for $g \ll g_0$.

The lens equation is

$$\theta_s = \theta - \frac{D_{LS}}{D_S} \alpha(\theta). \quad (3)$$

Here, θ_s and $\theta(= b/D_L)$ are the angular positions of the source and the image, and D_L, D_S and D_{LS}

³ We also examine other interpolation functions to study its dependence in section 4.

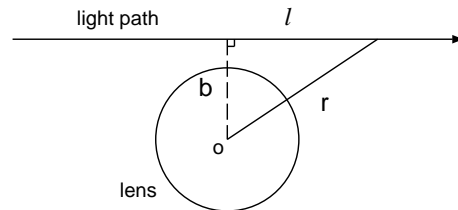


Fig. 1.— A schematic picture of the light ray passing through the lens.

²For example, Qin et al. (1995) assumed that the bending angle is 2 times larger than that for massive particles in the limit of $m \rightarrow 0$ by analogy with GR.

are the angular diameter distances between the observer, the lens and the source.⁴ The shear γ and the convergence κ are given by,

$$\gamma = \frac{1}{2} \left[\frac{\theta_s}{\theta} - \frac{d\theta_s}{d\theta} \right]; \quad 1 - \kappa = \frac{1}{2} \left[\frac{\theta_s}{\theta} + \frac{d\theta_s}{d\theta} \right] \quad (4)$$

We note that if the mass increases as $M \propto r^p$ with $p \geq 0$, the shear and the convergence decrease as

$$\begin{aligned} \gamma \propto \kappa \propto \theta^{p-2} & \quad \text{for } g \gg g_0, \\ \propto \theta^{p/2-1} & \quad \text{for } g \ll g_0, \end{aligned} \quad (5)$$

from Eqs.(1)-(4). The slopes of γ and κ for $g \gg g_0$ are steeper than that for $g \ll g_0$. This is because the gravitational force is proportional to $g_N^{1/2}$ for $g \ll g_0$, and hence the force decreases more slowly at larger distances. Comparing the slope in Eq.(5) with the observational data, we can test MOND.

3. Analysis with Cluster Data

We calculate the shear γ and the convergence κ based on the MOND theory for the three clusters, A1689, CL0024+1654, CL1358+6245, and the mean profile of 42 SDSS clusters. The mass profiles of these clusters have been measured by gravitational lensing for a wider range of angular diameters, and hence these clusters are an appropriate system to investigate the angle-dependence of the shear and the convergence.

3.1. A1689

Several authors have been studying the mass profile of the rich cluster A1689 at $z = 0.183$ ⁵ by strong and weak lensing, X-ray emission of gas, and dynamics of cluster members (e.g. Limousin et al. 2006 and references therein). The analysis of lensing data shows a small ellipticity ($\epsilon = 0.06$ in Halkola et al. 2006) and supports the assumption of quasi-circular symmetry (Umetsu, Takada & Broadhurst 2007). Andersson & Madejski (2004) provided the hot gas mass profile ($40\text{kpc} < r < 1\text{Mpc}$) directly determined by X-ray observational

data of the XMM-Newton telescope. Zekser et al. (2006) gave the galaxy mass profile ($20\text{kpc} < r < 260\text{kpc}$) from the surface brightness profile, assuming the constant mass-to-light ratio $8M_\odot/L_\odot$ (B-band). Fig.2(a) shows the mass profiles of the gas (dotted), the galaxies (dashed), and the sum of them (solid line). We also show the dark halo profile which will be needed to match the observational data (we will discuss this later).

Fig.2(b) shows the Newtonian gravitational acceleration g_N normalized to g_0 . As shown in this panel, the transition radius corresponding to $g_N = g_0$ (denoted by a horizontal dotted line) is 100 kpc for the gas + galaxies and is at 1000 kpc if the dark halo is added.

Broadhurst et al. (2005a) measured the distortions of 6000 red galaxies over $1' < \theta < 20'$ by the wide field camera, Suprime-Cam, of the Subaru telescope. Panel (c) shows their results, reduced shear profile $\gamma/(1-\kappa)$. The mean source redshift is $z_s = 1 \pm 0.1$ based on a photo-z estimation for deep field data. The solid line is the MOND theoretical prediction with $z_s = 1$. The gravitational source is only baryonic component (gas + galaxies). We note that for $\theta < 10'$ the solid line is clearly smaller than the data. This indicates that the gravitational force is too weak to explain the data. In order to solve this discrepancy, we need a very high mass-to-light ratio $\sim 200M_\odot/L_\odot$ ⁶. Even if the critical acceleration value g_0 increases, the discrepancy could not be resolved. In this case, the amplitude of the shear increases but the slope is too shallow to fit the data. MOND predicts shallower slope than $\gamma \propto \theta^{-1}$ for $g < g_0$ (since $p \geq 0$ in Eq.(5)), while the data in panel (c) clearly shows a steeper slope than this. Hence MOND cannot explain the data for any mass model and any acceleration parameter g_0 in the low acceleration region $g < g_0$.

We comment on the dependence of the source redshift z_s on the above results. The quantities γ and κ depend on z_s through a combination of D_{LS}/D_S , $\gamma \propto \kappa \propto D_{LS}/D_S$, from Eqs.(3) and (4). Hence these slopes are independent of z_s and the above results do not change. Furthermore the quantity D_{LS}/D_S is not sensitive to z_s for rela-

⁴We use the distance in the usual FRW (Friedmann-Robertson-Walker) model with $\Omega_M = 1 - \Omega_\Lambda = 0.3$ and $H_0 = 70\text{km/s/Mpc}$. The distance in MOND is almost the same as that in the FRW model (Bekenstein 2004).

⁵1' corresponds to 184kpc.

⁶The shear and the convergence are proportional to the mass-to-light ratio M/L for $g \gg g_0$, while $(M/L)^{1/2}$ for $g \ll g_0$.

tively low lens redshift ($z = 0.183$ for this cluster).

Previously, Aguirre, Schaye & Quataert (2001), Sanders (2003), and Pointecouteau & Silk (2005) reached the same conclusion as ours by studying temperature profiles of clusters. They indicated that the temperature data near the core is higher than the MOND prediction. Sanders (2003) noted that if the dark matter core were added, this discrepancy could be resolved. Following the previous studies, we include the dark halo to explain the observational data. We use the dark halo with a flat core :

$$M(< r) = M_0 \left(\frac{r}{r + r_0} \right)^3. \quad (6)$$

Here r_0 is the core radius and the density steeply decreases with proportional to r^{-4} for $r > r_0$: $\rho \propto (r + r_0)^{-4}$. We perform a χ^2 fit of the data in order to determine the parameters M_0 and r_0 . We also use the strong lens data (convergence field κ) from Broadhurst (2005b) in panel (d) in order to put a strong constraint on the core radius. They constructed the convergence field at $0.08' < \theta < 1.4'$ from 106 multiply images of 30 background galaxies by Hubble Space Telescope Advanced Camera for Surveys. The χ^2 is given by $\chi^2 = \sum_i (x_i - x_i^{data})^2 / \sigma_i^2$ where x_i is the reduced shear $\gamma / (1 - \kappa)$ and the convergence κ at the i -th angle, x_i^{data} is the data and σ_i is the standard deviation. The best fitted model is $M_0 = (1.1 \pm 0.1) \times 10^{15} M_\odot$ and $r_0 = 174 \pm 11$ kpc. These relative errors are less than 10% because of combining the strong and weak lensing data. The minimized χ^2 -value per degree of freedom (dof) is $\chi_{min}^2 / \text{dof} = 14.7/26$. The results are insensitive to the mass-to-light ratio. As shown in panels (c) and (d), this model (dashed line) fits the data well. The dashed line in panel (c) is steeper than the solid line, since $\theta < 5'$ ($\leftrightarrow r < 1000$ kpc) is the high acceleration region $g > g_0$ from panel (b) and hence the slope is steeper, as can be seen in Eq.(5).

We also try to fit the data by the other halo profiles : Navarro-Frenk-White (NFW) model $\rho \propto r(r + r_0)^{-2}$, Hernquist model $\rho \propto r(r + r_0)^{-3}$, isothermal (IS) with a core $\rho \propto 1/(r^2 + r_0^2)$. The minimum χ_{min}^2 are 29.8 for NFW, 22.6 for Hernquist, and 49.6 for IS with core which are larger than 14.7 for our model in Eq.(6). This is because the convergence data favor a flat core and

the shear data favor a steeply decreasing profile.

3.2. CL0024+1654

CL0024 is a rich cluster at $z = 0.395$ ($1'$ corresponds to 320 kpc) with a velocity dispersion of 1200 km s^{-1} (Dressler & Gunn 1992). Fig.3 (a) shows the mass profiles of the gas determined by the XMM-Newton telescope (Zhang et al. 2005), the galaxies with a mass-to-light ratio $8M_\odot/L_\odot$ (K-band) (Kneib et al. 2003), and the dark halo. For the larger radius > 2 Mpc the baryonic mass exceeds the dark halo mass. This is because we extrapolate the gas profile (fitted by isothermal β model for $r \lesssim 1$ Mpc) to the larger radius. Kneib et al. (2003) provided the reduced shear profile up to $10'$ measured by the Hubble Space Telescope as shown in panel (c). The mean source redshift is $z_s = 1.15$. We also use a constraint from an angular position of Einstein radius at $27''$ (denoted by a black square ■) based on an observation of giant arcs of distant galaxy at $z = 1.675$ (Smail et al. 1996; Broadhurst et al. 2000). The angular position of arcs is used to set a constraint on the enclosed mass within $27''$ ($= 140$ kpc). Similar to the previous case of A1689, for $\theta < 10'$ the solid line is smaller than the data, and we need the $\sim 30M_\odot/L_\odot$ to solve this discrepancy. The best fitted halo model is $M_0 = (2.0 \pm 0.4) \times 10^{14} M_\odot$ and $r_0 = 42 \pm 15$ kpc in Eq.(6) with $\chi_{min}^2 / \text{dof} = 5.6/7$. We caution that the core radius in the best fitting model $r_0 = 42 \pm 15$ is smaller than the inner most data point ($27'' = 140$ kpc), and hence this result has little meaning. It only means that the enclosed mass is $\sim M_0$ inside of 140 kpc.

3.3. CL1358+6245

The redshift of CL1358 is $z = 0.33$ and $1'$ corresponds to 280 kpc. Fig.3(a) shows the mass distribution of the gas (Arabadjis et al. 2002), the galaxies with a mass-to-light ratio $8M_\odot/L_\odot$ (V-band) (Hoekstra et al. 1998), and the dark halo. Hoekstra et al. (1998) presented the reduced shear profile ($\theta < 4'$) measured by HST as shown in panel (c). They fitted the data by the isothermal sphere model with the velocity dispersion of $780 \pm 50 \text{ km/s}$. The solid line is the MOND prediction with $D_{LS}/D_S = 0.62$. We need the $\sim 30M_\odot/L_\odot$ to fit the data if we assume only baryonic components. The best fitted model is $M_0 = (6.9 \pm 2.8) \times 10^{13} M_\odot$ and with $r_0 = 69 \pm 31$

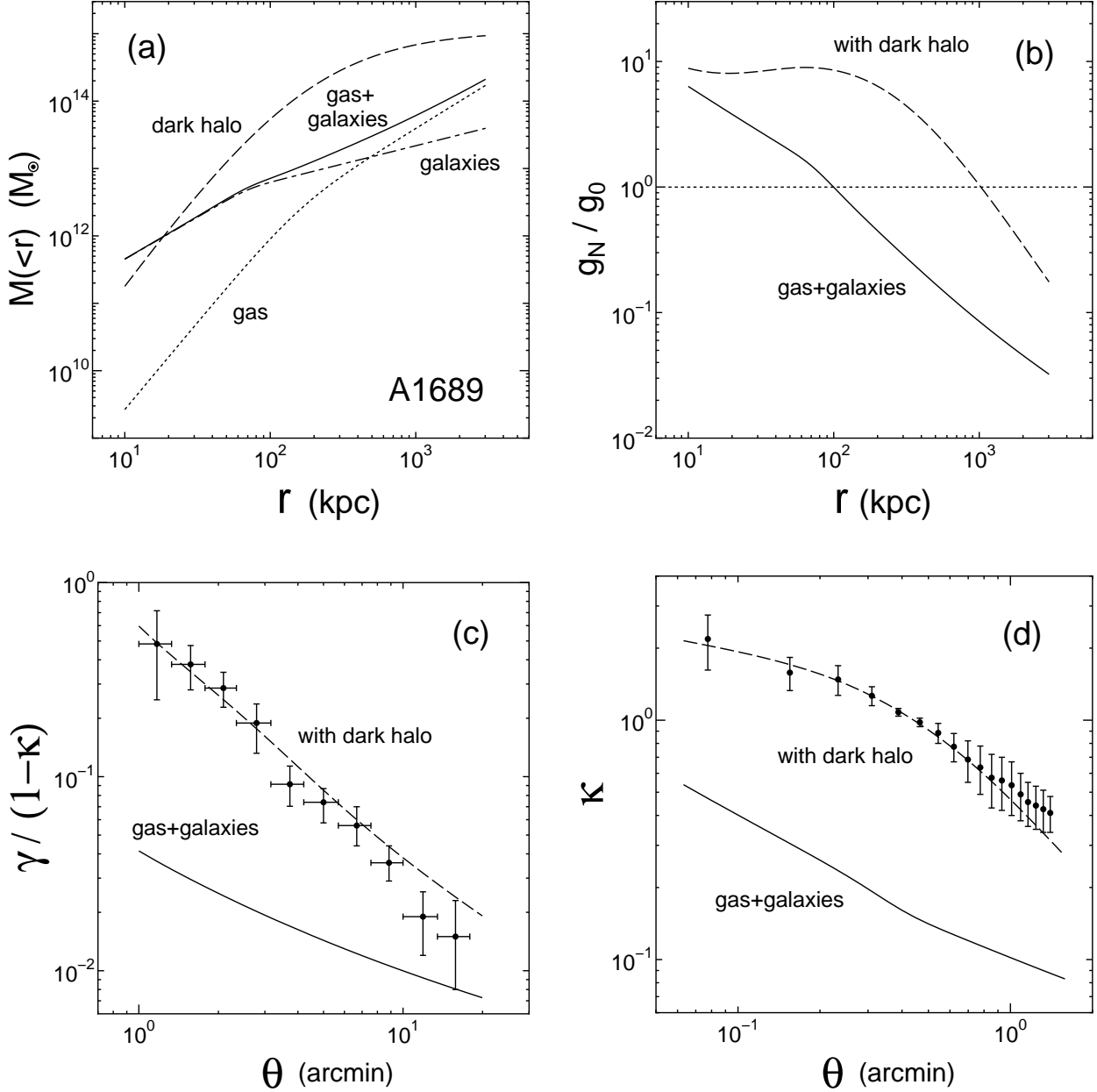


Fig. 2.— Results for the cluster A1689. The top left panel (a): The mass profiles of the gas (dotted line), the galaxies (dot-dashed line), the gas + galaxies (solid line), and the dark halo (dashed line). The quantity $M(< r)$ is the mass enclosed within the radius r . The top right panel (b): The Newtonian gravitational acceleration g_N normalised to g_0 for only baryonic components (gas + galaxies) (solid line) and all components (dark halo is added) (dashed line). The left bottom panel (c): The reduced shear $\gamma/(1 - \kappa)$ as a function of the angular radius. The data is from Broadhurst et al. (2005a). The solid line is the MOND prediction. On the dashed line, the dark halo is added. The right bottom panel (d): The convergence field κ from Broadhurst (2005b). From panels (c) and (d), the MOND cannot explain the data unless the dark halo is added, because the gravitational force is too weak near the core.

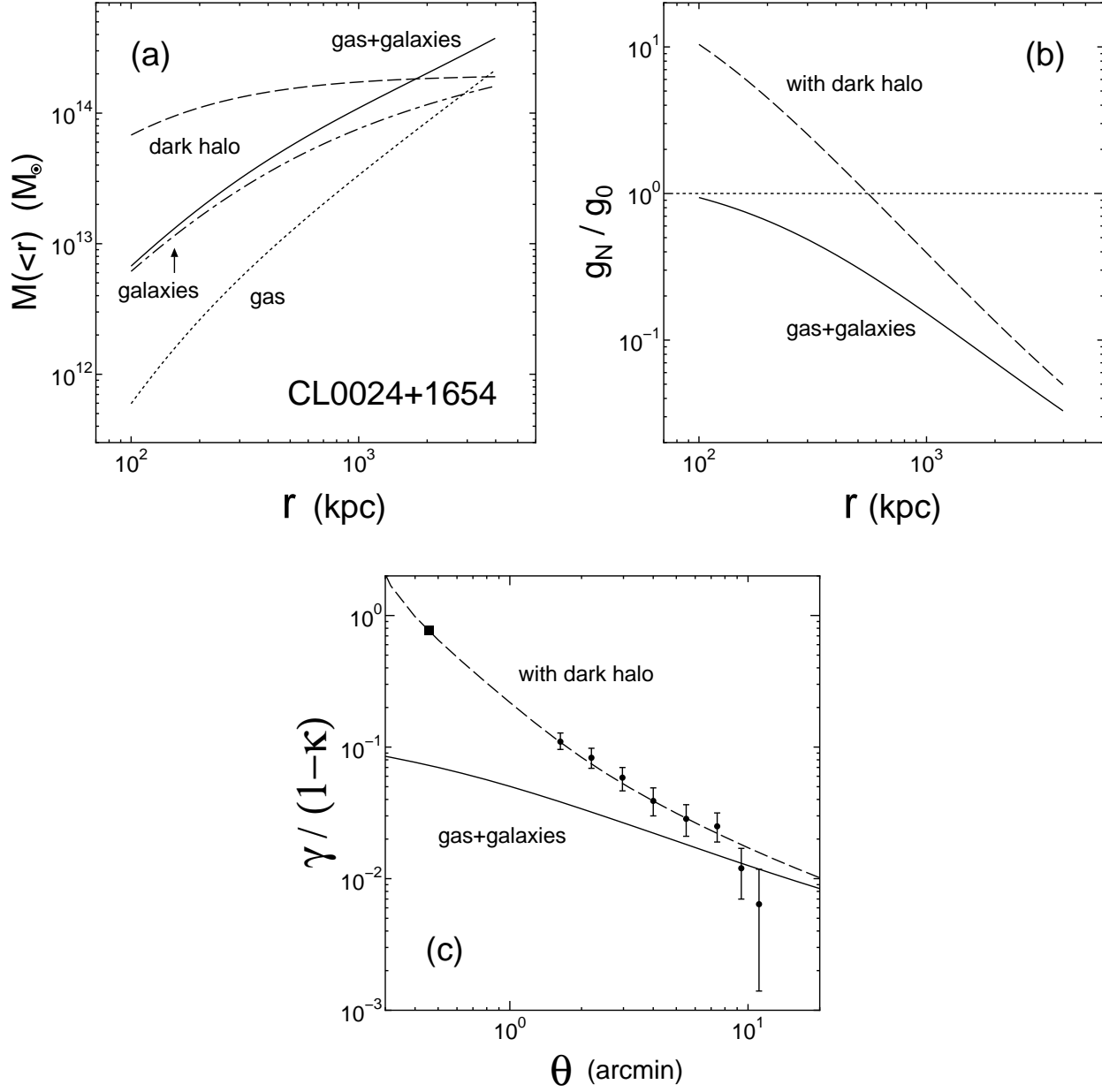


Fig. 3.— Same as Fig.2, but for the cluster CL0024+1654. The black square \blacksquare in panel (c) denotes the angular position of the Einstein ring.

kpc with $\chi^2_{min}/\text{dof} = 4.5/7$. Same as the case for CL0024, the core radius is smaller than the inner most data point. Although the discrepancy between the MOND prediction and the data is not so large in comparison with the previous cases, the dark halo model is better.

3.4. SDSS clusters

Sheldon et al. (2001) studied weak lensing of 42 clusters in SDSS data. They provided the mean shear of 42 clusters up to the radius of 2700 kpc as shown in Fig.5. The vertical axis is $\Sigma_{cr}\gamma$, where $\Sigma_{cr} = 1/(4\pi)D_S/(D_L D_{LS})$ is the critical surface density, and the horizontal axis is the projected radius⁷. Here, $\Sigma_{cr}\gamma$ does not depend on the source redshift. The data is well fitted by a power law with index -0.9 ± 0.3 (Sheldon et al. 2001). On the solid and dotted lines, we consider only the gas component, given by the isothermal beta model:

$$\rho(r) = \rho_0 \left[1 + \left(\frac{r}{r_c} \right)^2 \right]^{-3\beta/2}, \quad (7)$$

with $\beta = 0.6$, $r_c = 100$ kpc, $\rho_0/\rho_{cr} = 8000$ (solid line) and 800 (dotted line), here ρ_{cr} is the critical density at the present. As shown in the figure, the fit is poor. This is because the slope of the shear is $-3\beta/2 + 1/2 = -0.4$ for $g < g_0$ and it is flatter than the data. The dashed line is the dark halo model (given in Eq.(6)). The best fitted model is $M_0 = (3.8 \pm 1.1) \times 10^{13} M_\odot$ and $r_0 = 75 \pm 34$ kpc with $\chi^2_{min}/\text{dof} = 10.0/7$. The dashed line fits the data well.

4. Limit on Neutrino Mass

In previous studies, several authors assumed a massive neutrino with a mass of ~ 2 eV as the dark matter to explain the observational data (e.g. Sanders 2003; Skordis et al. 2006). In this section, we put a constraint on its mass from the weak lensing of clusters.

The neutrino oscillation experiments provide the mass differences between different species : $\Delta m_\nu^2 \lesssim 10^{-3} \text{eV}^2$. Here we consider massive neutrinos whose masses are much heavier than Δm_ν

⁷The quantity $\Sigma_{cr}\gamma$ is related to the surface density of the lens in GR : $\Sigma_{cr}\gamma = \Sigma(\leq R) - \Sigma(R)$.

and assume they are degenerate: they have (almost) the same mass, independent of species. Using the maximum phase space density h^{-3} , the maximum density of the neutrino dark halo is given by (Tremaine & Gunn 1979; Sanders 2003; 2007)⁸,

$$\rho_{\nu, max} = 2.3 \times 10^{-5} M_\odot/\text{pc}^3 \left(\frac{m_\nu}{2\text{eV}} \right)^4 \left(\frac{T}{\text{keV}} \right)^{3/2} \quad (8)$$

where T is the X-ray temperature : 9.0 ± 0.1 keV for A1689 (Andersson & Madejski 2004), 3.5 ± 0.2 keV for CL0024 (Zhang et al. 2005), and 7.2 ± 0.1 keV for CL1358 (Arabadjis et al. 2002).

For A1689, the core density of the neutrino halo is $\rho_c = 3M_0/(4\pi r_0^3)$ from Eq.(6). For CL0024 and CL1358, as we noted, the core radius r_0 in the best fitting model is smaller than the inner most data point. Hence, in order to put a conservative bound, we use the mean density inside the second innermost data point r_2 , $\rho_2 \equiv \rho(< r_2) = 3M(< r_2)/(4\pi r_2^3)$. Since $\rho_2 < \rho_c$, we obtain a lower bound of m_ν from Eq.(8). The results of ρ_c and ρ_2 are shown in Table 1. The lower row in each cluster is the case of another halo model $M(< r) = r^3/(r^3 + r_0^3)$ instead of Eq.(6). We try out this model in order to study the halo model dependence. For A1689 ρ_0 changes by a factor ~ 5 , and hence it depends on the halo profile. However for other clusters ρ_0 changes slightly (less than a factor 2), because there are no data point near the core radius r_0 and only M_0 is determined through the amplitude of the shear.

In Fig.6 we show the density ρ_0 vs. the temperature T to put a constraint on the neutrino mass. The dashed lines correspond to neutrino mass in Eq.(8). From the figure, the minimum neutrino mass is $2 - 3$ eV for CL0024 and CL1358. The above results are consistent with the previous X-ray measurements (Sanders 2003; Sanders 2007). Since the current limit is $m_\nu < 2$ eV from tritium β decay⁹, these values are comparable to or larger than this limit.

⁸Sanders (2007) recently revised his calculation and gave $\sim 1/3$ times smaller density than Sanders (2003). We confirm his calculation. Then the minimum neutrino mass is $\sim 3^{1/4} = 1.3$ times larger. Although Sanders (2007) is not yet published and there may be some ambiguities about the factor, we adopt his revised model.

⁹Particle Data Group Home Page : <http://pdg.lbl.gov/>

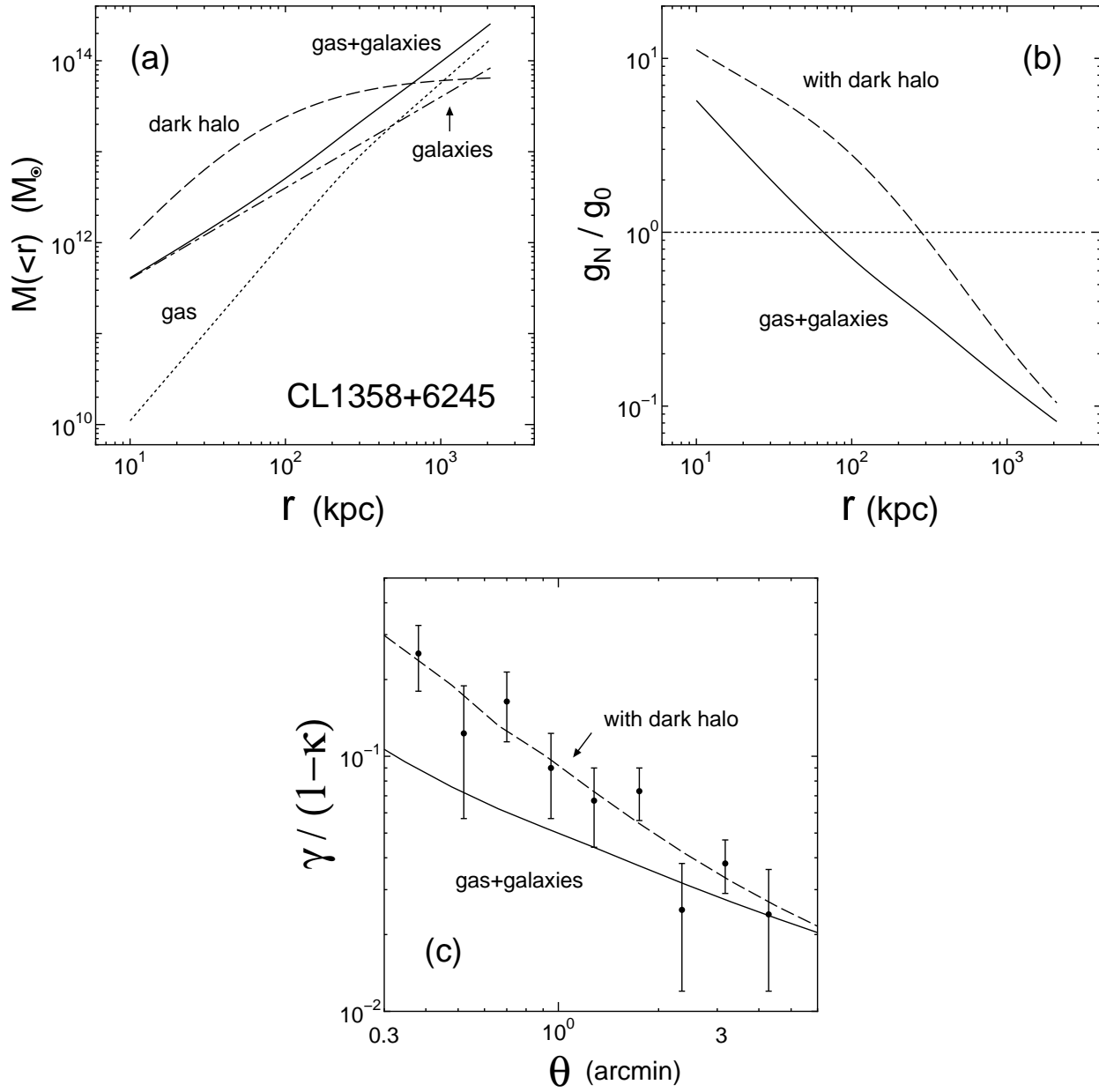


Fig. 4.— Same as Fig.2, but for the cluster CL1358+6245.

The mean density inside the innermost, not second innermost, data point is much higher than ρ_2 . The neutrino masses are 5–6 eV for CL0024 and 3–5 eV for CL1358 in this case. Hence there is an ambiguity about the definition of the central density for these clusters.

The core density of A1689 is highest and the minimum neutrino mass reaches 4–6 eV. To check our result, we compare the core density with the previous studies in GR. Since $g_N \sim 10 \times g_0$ for $r < r_0$ from Fig.2(b), GR is valid near the core. Halkola et al. (2006) gave central mass distribution by analyzing 107 multiple images of 32 background galaxies. Their mass distribution is consistent with Broadhurst et al. (2005b) (see Fig.17 of Halkola et al. (2006)). From a velocity dispersion of 1450 km/s and the core radius 77 kpc, the core density is $\rho_c = 0.01 M_\odot/\text{pc}^3$. This is roughly consistent with our result.

Allen (1998) suggests that the lensing core mass is generally a few times larger than X-ray core mass for non-cooling flow clusters (see also Clowe & Schneider 2001 in the case for A1689). Some ideas are proposed to explain the discrepancies : clusters are not in dynamical equilibrium, non-thermal pressure such as turbulent and magnetic pressure plays an important role, elongation of the cluster or substructures along a line-of-sight (e.g. Hattori, Kneib & Makino 1999). In fact, Lokas et al. (2006) show that A1689 is surrounded by a few substructures aligned along a line-of-sight, by studying the galaxy kinematics. CL0024 has a second mass clump which is separated at 3' from the center and has 30% of total cluster mass (Kneib et al. 2003). Jee et al. (2007) recently suggest that CL0024 would be the merging cluster in line-of-sight direction. These systematics would affect our results and change the neutrino mass limit by factor (since m_ν is not very sensitive to ρ_c , $m_\nu \propto \rho_c^{1/4}$ from Eq.(8)).

5. Results by Other Interpolation Functions

So far, we used a standard interpolation function $\tilde{\mu}(x) = x/\sqrt{1+x^2}$ alone. However the standard $\tilde{\mu}$ is not consistent with TeVeS (Bekenstein 2004). In this section, we also examine other interpolation functions, Bekenstein's toy model in TeVeS $\tilde{\mu}(x) = 4x/(1 + \sqrt{1+4x})^2$

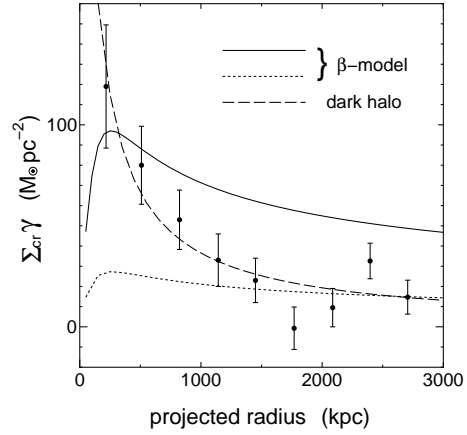


Fig. 5.— The mean shear of 42 SDSS clusters. The solid and dotted lines are the beta models, and the dashed line is the dark halo model.

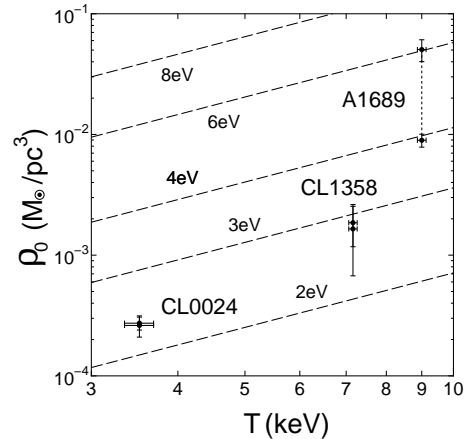


Fig. 6.— The central density vs. the X-ray temperature. The density ρ_0 is the core density for A1689, and mean density inside of the second innermost data point for CL0024 and CL1358. There are two points with error bars for each cluster corresponding to the two density profile models in Table.1. The vertical dotted line connecting these pairs represents the systematic uncertainty in the density model. The dashed lines correspond to minimum neutrino mass in Eq.(8).

TABLE 1
BEST FITTING MODEL FOR DARK HALO PROFILE AND CENTRAL DENSITY

| | M_0 (M_\odot) | r_0 (kpc) | ρ_0 (M_\odot/pc^3) |
|--------|--------------------------------|--------------|------------------------------------|
| A1689 | $(1.1 \pm 0.1) \times 10^{15}$ | 174 ± 11 | $(5.1 \pm 1.0) \times 10^{-2}$ |
| | $(5.1 \pm 0.3) \times 10^{14}$ | 239 ± 9 | $(9.0 \pm 1.1) \times 10^{-3}$ |
| CL0024 | $(2.0 \pm 0.4) \times 10^{14}$ | 42 ± 15 | $(2.6 \pm 0.6) \times 10^{-4}$ |
| | $(1.7 \pm 0.2) \times 10^{14}$ | 147 ± 19 | $(2.8 \pm 0.3) \times 10^{-4}$ |
| CL1358 | $(6.9 \pm 2.8) \times 10^{13}$ | 69 ± 31 | $(1.7 \pm 1.0) \times 10^{-3}$ |
| | $(4.0 \pm 1.1) \times 10^{13}$ | 127 ± 27 | $(1.9 \pm 0.7) \times 10^{-3}$ |

NOTE.—The best fitting parameters M_0 and r_0 . The density ρ_0 is the core density ρ_c for A1689 and the mean density inside the second innermost data point ρ_2 for the others. The upper row is the case of the halo profile $M(< r) = M_0 r^3 / (r + r_0)^3$ given in Eq.(6), while the lower row is $M(< r) = M_0 r^3 / (r^3 + r_0^3)$.

and simple model $\tilde{\mu}(x) = x/(1+x)$ in Famaey & Binney (2005), in order to study the robustness of our results. Since the clusters have $g_N \approx g_0$ from Figs.2-4 (b), our conclusions may depend on the choice of $\tilde{\mu}$.

In Fig.7, we show the MOND predication for A1689 for the three types of $\tilde{\mu}(x)$. The solid line is the standard model, the dashed line is the Bekenstein's toy model (B04), and the dotted line is the Famaey & Binney's model (FB). The standard model predicts the lowest value, because $\tilde{\mu}(x)$ is highest at $x \sim 1$. B04 and FB show several times 10% higher values than the standard model.

The minimum neutrino mass only $\sim 10\%$ changes and the choice of $\tilde{\mu}$ is not crucial.

6. Conclusion

We have studied the weak lensing of galaxy clusters in MOND. We calculate the shears and the convergences of the background galaxies for three clusters (A1689, CL0024, CL1358) and the mean profile of 42 SDSS clusters, and compare them with the observational data. It turns out that the MOND cannot explain the data irrespective of g_0 unless a dark matter halo is added. We also examine the three types of interpolation function, but the conclusion does not change. The

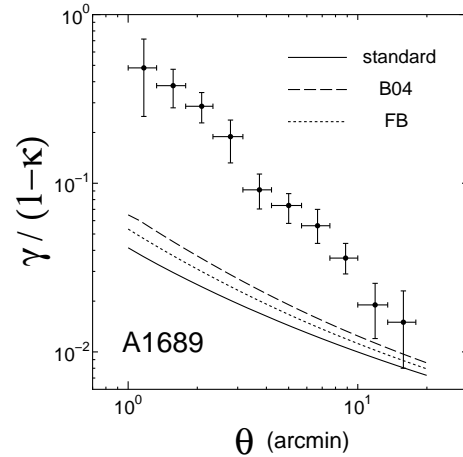


Fig. 7.— The MOND predications for A1689 for the three interpolation functions. The solid line is the standard model $\tilde{\mu}(x) = x/\sqrt{1+x^2}$, the dashed line is the Bekenstein's toy model (B04) $\tilde{\mu}(x) = 4x/(1 + \sqrt{1+4x})^2$, and the dotted line is the Famaey & Binney's model (FB) $\tilde{\mu}(x) = x/(1+x)$.

above results are consistent with those of previous studies (e.g. Aguirre, et al. 2001; Sanders 2003). If the dark halo is composed of massive neutrinos, its minimum mass is 4 – 6 eV for A1689 and 2 – 3 eV for CL0024 and CL1358. However our results still depends on the dark halo model and inner data points. Even for A1689, the system with the most constraining data, the systematic is more important than random errors as shown in Fig.6. In addition, there are some systematic uncertainties such as an elongation of cluster along line-of-sight. These effects would reduce the minimum mass by a factor of ~ 2 . In the low acceleration region ($g_N \lesssim g_0$), the external gravitational field becomes important and would affect the outer shear profile (Bekenstein & Milgrom 1984; Wu et al. 2007).

In conclusion, the more careful study is necessary to put a stringent constraint, for example, a combination of the weak and strong lensing, X-ray gas and galaxy dynamics. However, it is beyond the scope of this paper and we will study as an future work. Even so, at present, we find that there is some tension between the lower bound of neutrino mass in neutrino dark halo model in MOND and the upper bound by experiments.

We would like to thank Takashi Hamana for useful comments and discussions. We also thank the anonymous referee for helpful comments to improve the manuscript. TC was supported in part by a Grant-in-Aid for Scientific Research (No.17204018) from the Japan Society for the Promotion of Science and in part by Nihon University.

REFERENCES

- Aguirre, A., Schaye, J. & Quataert E. 2001, *ApJ*, 561, 550
- Aguirre, A. 2003, in *Proc. the IAU Symposium 220 "Dark Matter in Galaxies"*, ed. by S. Ryder, D.J. Pisano, M. Walker and K. Freeman, 17
- Allen, S.W. 1998, *MNRAS*, 296, 392
- Andersson, K.E. & Madejski, G.M. 2004, *ApJ*, 607, 190
- Angus, G.W., Famaey, B. & Zhao, H.S. 2006, *MNRAS*, 371, 138
- Angus, G.W., Shan, H.Y., Zhao, H.S. & Famaey, B. 2007, *ApJ*, 654, L13
- Angus, G.W. & McGaugh, S.S. 2007, arXiv:0704.0381, submitted to *MNRAS*
- Arabadjis, J.S. Bautz, M.W. & Garmire, G.P. 2002, *ApJ*, 572, 66
- Bekenstein, J.D. & Milgrom, M. 1984, *ApJ*, 286, 7
- Bekenstein, J.D. 2004, *Phys. Rev. D*, 70, 083509
- Broadhurst, T., Huang, X., Frye, B. & Ellis, R. 2000, *ApJ*, 534, L15
- Broadhurst, T. et al. 2005a, *ApJ*, 619, L143
- Broadhurst, T. et al. 2005b, *ApJ*, 621, 53
- Chen D.-M. & Zhao, H.S. 2006, *ApJ*, 650, L9
- Chiu, M.-C., Ko, C.-M. & Tian, Y. 2006, *ApJ*, 636, 565
- Clowe, D. & Schneider, P. 2001, *A&A*, 379, 384
- Clowe, D. et al. 2006, *ApJ*, 648, L109
- Dodelson, S. & Liguori, M. 2006, *Phys. Rev. Lett.*, 97, 231301
- Dressler, A. & Gunn, J.E. 1992, *ApJS*, 78, 1
- Famaey, B. & Binney, J. 2005, *MNRAS*, 363, 603.
- Famaey, B., Angus, G.W., Gentile, G. & Zhao, H.S. 2007, arXiv:0706.1279, submitted to *A&A*
- Feix, M., Fedeli, C., and Bartelmann, M. 2007, arXiv:0707.0790, submitted to *A&A*
- Gavazzi, R. 2002, *New A Rev.*, 46, 783
- Halkola, A., Seitz, S., & Pannella, M. 2006, *MNRAS*, 372, 1425
- Hattori, M., Kneib, J.P. & Makino, N. 1999, *Prog.Theor.Phys.Suppl.*, 133, 1
- Hoekstra, H., Franx, M., Kuijken, K., & Squires, G. 1998, *ApJ*, 504, 636
- Jee, M.J., et al. 2007, *ApJ*, 661, 728
- Kneib, J.P. et al. 2003, *ApJ*, 598, 804
- Limousin et al. 2006, astro-ph/0612165
- Lokas et al. 2006, *MNRAS*, 366, L26

- Milgrom, M. 1983, ApJ, 270, 365
- Mortlock, D.J. & Turner, E.L. 2001, MNRAS, 327, 552
- Mortlock, D.J. & Turner, E.L. 2001, MNRAS, 327, 557
- Pointecouteau, E. & Silk, J. 2005, MNRAS, 364, 654
- Qin, B., Wu, X.P. & Zou, Z.L. 1995, A&A, 296, 264
- Sanders, R.H. & McGaugh S.S. 2002, ARA&A, 40, 263
- Sanders, R.H. 2003, MNRAS, 342, 901
- Sanders, R.H. 2007, submitted to MNRAS, astro-ph/0703590
- Sheldon, E.S. et al. 2001, ApJ, 554, 881
- Slosar, A., Melchiorri, A. & Silk, J.I. 2005, Phys. Rev. D, 72, 101301
- Skordis, C. 2005, submitted to Phys. Rev. D, astro-ph/0511591
- Skordis, C., Mota, D.F., Ferreira, P.G., & Boehm C. 2006, Phys. Rev. Lett., 96, 011301
- Smail, I. et al. 2006, ApJ, 469, 508
- Tremaine, S. & Gunn, J.E. 1979, Phys. Rev. Lett., 42, 408
- Umetsu, K., Takada, M. & Broadhurst, T. 2007, submitted to Mod. Phys. Lett. A, astro-ph/0702096
- Zekser, K.C. et al. 2006, ApJ, 640, 639
- Zhang, Y.-Y. et al. 2005, A&A, 429, 85
- Zhao, H.S. et al. 2006, MNRAS, 368, 171
- White, M. & Kochanek, C.S. 2001, ApJ, 560, 539
- Wu, X. et al. 2007, arXiv:0706.3703, submitted to ApJ